

HEAT TRANSFER COEFFICIENTS ON LONGITUDINAL
FINNED SURFACES

by
A.R. McKay

Thesis submitted in partial fulfillment
of the requirements for the degree of
Master of Engineering

Department of Mechanical Engineering
McGill University
Montreal
April 1961

SUMMARY

Tests have been conducted to determine heat transfer coefficients on the surface of fins. The range of Reynolds numbers covered, based on the distance from hydrodynamic leading edge are 1.85×10^5 to 1.43×10^6 .

Expressions for heat transfer film coefficients based on experimental data have been obtained in terms of fin flow-channel centre-line velocity for the case of fins with a height of 1.5 inch, with spacings of $3/8$, $1/2$, $5/8$ and $3/4$ inch, using a film coefficient transducer designed specifically for this purpose.

The experimental results indicate that film coefficients are dependent on film geometry and suggest the presence of an optimum condition caused by the effect of vortices resulting from secondary flows within the fin flow-channel.

ACKNOWLEDGEMENTS

The author wishes to express his sincere gratitude to Professor J.W. Stachiewicz for his advice and guidance during this investigation and in the preparation of this thesis.

The assistance of the Mechanical Engineering Department technical staff in particular Mr. Frank Kadlec in the construction of the experimental apparatus and Mr. I. Wygnanski for his help during the tests, is acknowledged.

Thanks are due to Miss J. Lacroix and Miss H. Tucker for the typing, and Mrs. A.J. Patten for the printing of this thesis.

The financial assistance of the National Research Council is gratefully acknowledged.

CONTENTS

	Page
SUMMARY	i
ACKNOWLEDGEMENTS	ii
CONTENTS	iii
LIST OF ILLUSTRATIONS	iv
NOMENCLATURE	v
INTRODUCTION	1
THEORY	
Basic Fin Theory	4
Work of Ghai and Jakob	5
Film Coefficient Element	7
Effect of Unheated Starting Lengths	13
FILM COEFFICIENT TRANSDUCER	
Construction of Elements	15
Calibration a) resistance-temperature	17
b) flat plate	20
Control of Elements	23
PROCEDURE AND RANGE OF TESTS	27
RESULTS AND DISCUSSION	28
CONCLUSIONS AND RECOMMENDATIONS	36
REFERENCES	39
APPENDIX I - General Apparatus	41

LIST OF ILLUSTRATIONS

	Page
Plate 1	
1 Conductor Pattern	45
2 Film Coefficient Transducer	45
3 Boundary Layer Control Suction Slots	46
4 Wind Tunnel Working Section	46
5 Control Panel	47
6 Wind Tunnel	47
7 3/8 inch Spacing Fin System	48
8 Velocity Traverse Mechanism	48
Figure 1	
Fin and Small Element of Volume Bounded by Isothermals and Heat Flow Boundaries.	49
2 Heat Transfer Fin and Heating Elements	50
3 Control and Measuring Circuits	51
4 Typical Flow Profile at Inlet to Fins	52
5 Film Coefficient Versus Velocity (3/8 inch fin spacing)	53
6 Film Coefficient Versus Velocity (1/2 inch fin spacing)	54
7 Film Coefficient Versus Velocity (5/8 inch fin spacing)	55
8 Film Coefficient Versus Velocity (3/4 inch fin spacing)	56
9 Boundary Region at the Intersection of Two Planes	57
10 Secondary Flows in a rectangular Channel	57
11 Curves of Constant Velocity in Fin Channel	58

NOMENCLATURE

A	coefficient, dimensionless	
A _O	coefficient, dimensionless	
A _S	heat transfer area	ft ²
a	exponent, dimensionless	
b	fin thickness	ft
C _O	coefficient, dimensionless	
c	exponent, dimensionless	
C _p	specific heat	BTU.LB. ⁻¹ °F ⁻¹
E	potential difference	Volts
h	convective film coefficient	BTU.HR ⁻¹ FT ⁻² °F ⁻¹
I	Current	Amperes
K	coefficient, dimensionless	
k	thermal conductivity	BTU.HR ⁻¹ FT ⁻¹ °F ⁻¹
L	fin height	FT.
m	exponent, dimensionless	
n	exponent, dimensionless	
p	exponent, dimensionless	
q ₁	heat entering volume element by conduction	BTU.HR ⁻¹
q ₂	heat leaving volume element by conduction	BTU.HR ⁻¹
q _c	heat leaving volume element by convection	BTU.HR ⁻¹
q _r	heat leaving volume element by radiation	BTU.HR ⁻¹
q _{gen}	heat generated within volume element	BTU.HR ⁻¹

R	resistance	OHMS
S	fin spacing	FT
T	temperature	°F or °C
T _e	element temperature	°F or °C
T _s	fluid stream temperature	°F or °C
V	velocity	FT.SEC ⁻¹
x	length in direction of flow	FT
y	length along fin surface normal to x	FT
α	temperature coefficient	OHMS °C ⁻¹
ρ	density	LBS.FT ⁻³
μ	absolute viscosity	LBS.FT ⁻¹ SEC ⁻¹
ν	kinematic viscosity	FT ² .SEC ⁻¹

DIMENSIONLESS GROUPINGS

Reynolds number
$$N_{Re} = \frac{\rho V x}{\mu} = \frac{V x}{\nu}$$

Prandtl number
$$N_{Pr} = \frac{C_p \mu}{k}$$

Nusselt number
$$N_{Nu} = \frac{h x}{k}$$

INTRODUCTION

When dealing with forced convective heat transfer from fins or extended area surfaces, the usual simplifying assumption made is that the value of the coefficient of convective heat transfer does not change with position on the surface. Due to the viscous drag experienced by the fluid flowing through a system of fins, boundary layers build up on the surfaces and the interaction of these boundary layers cause a velocity distribution from fin tip to fin root as well as across the flow channel between successive fins. This velocity distribution causes variations in the local value of the convective heat transfer coefficient.

The influence of the boundary layer for the case of a cylinder with circular fins has been covered in papers by Lemmon, Colburn and Nottage¹ and by McAdams, Drexel and Goldey². Neither of these papers attempted to determine the variation of the film coefficient with position on the fin surface. Harper and Brown³ and K.A. Gardner⁴ have analyzed a variety of fin geometries with respect to fin performance considering average values of film coefficients over the surface rather than local values based on position relative to fin height and distance from hydrodynamic starting edge.

Ghai and Jakob⁵ attacked the problem using a system of straight parallel fins which were heated at their bases. Correlations of local film coefficients with fin geometry based on fluid velocity at inlet to the fin system were obtained. The correlations could not be based on local values of velocity because of limitations in the experimental apparatus.

A more exact analysis not only requires the evaluation of fin performance based on average or overall values of film coefficient, but must also consider the effect of the variation of the local value of coefficient with position in order to obtain the average. Furthermore, the interrelation of fin geometry and its effect on the local value of film coefficient must also be considered. As a limited amount of work has been done in the determining of the variations of film coefficient with position on fins and the interrelation of this variation with system geometry and fluid properties, it was decided to undertake investigation in the field.

All previous research considered fins heated at the base. Hence the temperature gradient along the surface, which varies with fin material and position, had to be established in order to evaluate the film coefficient to obtain either the local or average values. It was decided that a more direct approach should be adopted. By considering an isothermal surface, the effects of material conductance and associated temperature profile

would be removed and the local value of film coefficient could be obtained directly.

The object of this work is of two-fold nature. Firstly, to develop an experimental technique to measure the local heat transfer coefficient and secondly to investigate the possibility of a correlation for heat transfer coefficients incorporating such parameters as geometric configuration and local fluid properties. It is the object of this thesis to deal with the first of the above mentioned problems and to evaluate the possibility of its application to the solution of the second.

THEORY

Basic Fin Theory

The fin shown in Figure 1 represents one fin of a system of fins heated at the base. A small element of volume is bounded by isothermals in the X-direction across which heat flows and by heat flow boundaries in the Y-direction across which there is no flow of heat. A heat balance for the element may be set up in the following manner:

$$q_1 - q_2 - q_c - q_r = 0 \quad \dots\dots (1)$$

$$\text{where: } q_1 = -k b x \frac{dT}{dy} \quad \dots\dots (2)$$

$$q_2 = -k b (x + \Delta x) \frac{d}{dy} (T + \Delta T)$$

expanding the terms in brackets and assuming $(\Delta y)^2$ may be neglected

$$q_2 = -k b \left(x \frac{dT}{dy} + x \frac{d^2 T}{dy^2} \Delta y + \frac{dx}{dy} \frac{dT}{dy} \Delta y \right) \dots (3)$$

q_r , the rate of heat leaving the volume element due to radiation may be neglected provided that the element temperature is kept low with respect to the stream temperature, hence:

$$q_r = 0 \quad \dots\dots\dots (4)$$

q_c , the heat leaving the element by convection under the influence of the film coefficient "h" on both surfaces

exposed to the flow may be expressed as follows:

$$q_c = 2h \left(x + \frac{\Delta x}{2} \right) \Delta y (T_e - T_s)$$

expanding and neglecting the $\frac{\Delta x \Delta y}{2}$ term

$$q_c = h (2 x \Delta y) (T_e - T_s) \quad \dots\dots (5)$$

combining equations (1), (2), (3), (4) and (5)

$$k b \left(x \frac{d^2 T}{dy^2} \Delta y + \frac{dx}{dy} \frac{dT}{dy} \Delta y \right) = 2 x \Delta y h (T_e - T_s) \quad \dots\dots (6)$$

$$\frac{d^2 T}{dy^2} + \frac{1}{x} \frac{dx}{dy} \frac{dT}{dy} - \frac{2h}{kb} (T_e - T_s) = 0 \quad \dots\dots (6a)$$

Work of Ghai and Jakob

By expressing equation (6) in the form of finite differences

$$\frac{\Delta^2 T}{\Delta y^2} + \frac{1}{x} \frac{\Delta x}{\Delta y} \frac{\Delta T}{\Delta y} = \frac{2h}{kb} (T_e - T_s) \quad \dots\dots\dots (7)$$

calculation of local values of the film coefficient "h" is possible by obtaining first and second derivatives graphically from an accurately known temperature distribution on the fin surface. It is this approach that was used by Ghai and Jakob⁵, who obtained the necessary temperature distribution from a fin surface instrumented with a large number of thermocouples.

Ghai⁶ expressed the local film coefficients h_{xy} in the form of Nusselt numbers defined as:

$$N_{Nu_{xy}} = \frac{h_{xy} x}{k_f} \dots\dots\dots (8)$$

where k_f , the thermal conductivity of the fluid film, was taken at the mean film temperature.

The Nusselt number was considered to be a function of the free stream Reynolds number,

$$N_{Re} = \frac{V_a x}{\nu_a} \dots\dots\dots (9)$$

where both the velocity and viscosity values were based on free stream or inlet conditions.

A practical expression of the functional relationship between the Nusselt and Reynolds numbers was given as:

$$N_{Nu_{xy}} = C_o (N_{Re})^n \left[1 - C_1 \left(\frac{L}{S} \right)^m \left(\frac{L-y}{L} \right)^p \right] \dots (10)$$

As the film coefficient in the y direction was of major importance a mean coefficient defined as:

$$h_{my} = \frac{1}{x} \int_{x=x_{st}}^{x=x} h_{xy} dx \dots\dots\dots (11)$$

was employed. x_{st} is the distance from the leading edge of the fin to the edge of the fin section where heat is supplied. By substitution in equation (10):

$$N_{Nu_{my}} = C_o (N_{Re})^n \left[1 - C_1 \left(\frac{L}{S} \right)^m \left(\frac{L-y}{L} \right)^p \right] \dots\dots (12)$$

Using experimental data Ghai⁶ plotted the various parameters in non-dimensional form and obtained values for the constants C_0 and C_1 and the powers n , m and p . The numerical forms of equation (12) obtained were:

for the laminar region

$$N_{Nu_{my}} = 0.7 N_{Re}^{0.5} \left[1 - 0.35 \left(\frac{L}{S} \right)^{1/3} \left(\frac{L-y}{L} \right)^2 \right] \dots \dots (13)$$

for the turbulent region:

$$N_{Nu_{my}} = 0.03 N_{Re}^{0.8} \left[1 - 0.23 \left(\frac{L}{S} \right)^{1/2} \left(\frac{L-y}{L} \right)^{3/2} \right] \dots \dots (14)$$

Film Coefficient Element

Equation (6) was developed for the case of a fin heated at the base. No term is included to cover the possibility of heat generation within the element of volume itself. Including such a term in equation (6) we have:

$$\begin{aligned} q_{gen} + k b \left(x \frac{d^2 T}{dy^2} \Delta y + \frac{dx}{dy} \frac{dT}{dy} \Delta y \right) \\ = 2 x (\Delta y) h (T_e - T_s) \dots \dots (15) \end{aligned}$$

where q_{gen} is the heat generated within a small element of volume.

By appropriate distribution of the heat generated by the large number of volume elements which make up the fin, it is possible to reduce the temperature gradient across each volume element to zero. This would result in a fin with a constant temperature or isothermal surface. The first and second derivative terms in equation (15) would disappear. With heat being generated from within the fin itself that heat which was previously supplied at the base is no longer required and equation (15) becomes:

$$q_{\text{gen}} = 2 h (x) (\Delta y) (T_e - T_s) \quad \dots\dots\dots (16)$$

The product $2 (x) (\Delta y)$ is equal to A_s the area of both faces of the volume element exposed to the fluid flow. The film coefficient may then be expressed in terms of the generated heat, the area and the temperature difference:

$$h = \frac{q_{\text{gen}}}{A_s(T_e - T_s)} \quad \dots\dots\dots (17)$$

If a volume element of the fin under consideration were heated by means of an electrical conductor then for a fixed area and temperature difference equation (17) could be expressed as:

$$h = K E I \quad \dots\dots\dots (18)$$

where E and I are the voltage and current respectively, applied to the conductor and K is a constant incorporating

the area, the temperature difference and the conversion factor from watts to B.T.U.'s per hour.

The accuracy with which the film coefficient may be calculated by the method of Ghai⁶, using equation (7) depends on the accuracy of the measured fin temperature distribution and also on the graphically determined derivatives of temperature with distance obtained from this temperature distribution. The method as suggested by equation (18) does not depend on graphically determined values, but on directly recorded measurements of voltage and current supplied to the conductor heating the volume element. The accuracy of the film coefficient obtained with equation (18) would depend on the accuracy of the measured values of voltage and current, the evaluation of the heat transfer area and the degree to which the element temperature could be maintained constant.

The fin shown in Figure 2 has surfaces which are made up of a series of strip heating elements. Each element consists of a strip conductor ABCD on one face of the fin connected to an exactly similar strip conductor EF on the opposite face by a connection through the fin at E and D. With connections at A and F it is possible to pass a current along the path ABCDEF through both strip conductors. Heat will be developed as the strip conductors have resistance and though this heat is developed on both surfaces it is analogous to the case where heat is generated within the volume of fin

material contained between the strip conductors. Furthermore as both strips are identical and the same current passes through them, each strip will assume the same temperature provided flow conditions are the same along both surfaces.

The heat generated by the element not only flows under the influence of the film coefficient to the fluid passing over the fin surface, but will also flow through the fin material in both the x and y directions. By locating similar elements above and below the one under consideration and operating these elements at the same temperature, no temperature difference will exist and hence no heat will flow in the y direction. Heat flow in the x direction is arrested in a similar manner. Sections at each end of the strip conductor shown as AB and CD in Figure 2 act as guard sections for the volume of fin material contained between the strip conductors from B to C.

The heat generated between B and C must then flow from the element to the fluid. The rate of this heat flow will be governed by the film coefficient existing at the surface. Thus by measuring the current flow through the heating element and the potential difference between B and C the amount of heat generated, which is a direct measure of the film coefficient, may be calculated.

As each of the heating elements which make up the surface of the fin shown in Figure 2, must be at the same temperature and this temperature kept constant, the accurate determination of the element temperature is of prime importance. Since the heating elements are electrical conductors, their resistance may be readily calculated from the measured values of the current through the element and the potential difference across that section of the element used in the determination of the film coefficient, by the following relation:

$$R = \frac{E}{I} \quad \text{..... (19)}$$

The variation of resistance with temperature of an electrical conductor may be expressed in the following manner:

$$R_t = R_o (1 + \alpha t) \quad \text{..... (20)}$$

where R_t is the value of the resistance at some temperature t , R_o is the resistance at a chosen reference temperature, t is the number of degrees above or below this reference temperature. The temperature coefficient, α , is a constant which depends on the conductor material and the chosen reference temperature. By suitable choice of the reference temperature, t will become T_e the element temperature.

Combining equations (19) and (20), we have a convenient expression for the element temperature in terms of the measured current I the potential difference E and the constants R_0 and α . Hence;

$$T_e = \frac{(E/I) - R_0}{R_0 \alpha} \dots\dots\dots (21)$$

Through the use of equation (21) and equation (18) we are able to establish the element temperature and evaluate the film coefficient by the same two measured variables E and I. By appropriate design, we are able to construct the fin in such a way that there are a number of individually controlled heating elements from fin tip to fin root as indicated by Figure 2. Thus we are able to evaluate the film coefficient at various points in the y direction on the fin surface.

Local coefficients are desired, and it is necessary that the heating elements have sufficient length in the x direction for their electrical resistance to be significant. Film coefficients as evaluated by equation (16) are actually coefficients at a position y and a mean value over the length (x direction) of the element. This coefficient was previously designated as h_{my} in equation (11).

Effect of Unheated Starting Length

A further factor must also be considered. The thermal boundary layer does not start at the leading edge of the fin as does the hydrodynamic boundary layer. The heating elements are placed at some distance downstream from the leading edge in a region of fully developed flow. The effect of unheated starting length must then be considered.

The effect of unheated starting length on film coefficients has been investigated by Scesa⁷, Rubesin⁸ and Jakob⁹. The relation advanced by Scesa⁷ best summarizes the results of other researchers in the field.

$$N_{Nu_x} = 0.0289 N_{Pr}^{1/9} (N_{Re_x})^{0.8} \left[1 - \left(\frac{x_o}{x} \right)^{.9} \right]^{-\frac{1}{9}} \quad \text{..... (22)}$$

The above relation considers the case of the flat plate and is analogous to the case of the fin if the velocity at the centerline of the flow channel is used in the Reynolds Number determination. Equation (22) may then be expressed as;

$$\frac{h_{xy} x}{k} = 0.0289 (N_{Pr})^{\frac{1}{9}} \left(\frac{\rho v_{xy} x}{\mu} \right)^{0.8} \left[1 - \left(\frac{x_o}{x} \right)^{.9} \right]^{-\frac{1}{9}} \quad \text{..... (23)}$$

Since the film coefficient as determined by equation (18) is a mean value or h_{my} , this value may be substituted in equation (11) with the expression

for h_{xy} from equation (23) to yield a value for x at which h_{my} occurs.

$$h_{my} = \frac{1}{x} \int_{x=x_{st}}^{x=x} h_{xy} dx \quad \dots (11)$$

It is on the value of x at which h_{my} occurs that the correlations of Nusselt and Reynolds numbers will be based.

FILM COEFFICIENT TRANSDUCER

Construction of Elements

The section of the fin containing the heating elements used for the film coefficient determination was constructed using a technique similar to that used in the electronics industry for "etched circuits".

A double clad laminate consisting of a glass-base insulating material with a sheet of 0.0015 inch thick electrolytically pure copper bonded to one face, and a sheet of 0.020 inch copper bonded to the other face, made up the basic material for the heating element construction. The double clad laminate, or resulting "sandwich", was slightly less than 1/16 inch in overall thickness.

Eight separate heating elements, 2 inches in length, equispaced from fin tip to fin root to make up an overall fin height of 1.5 inches were used on each side of the fin surface. The grid pattern for each heating element was etched on the 0.0015 inch copper face of the laminate and the appropriate conductor pattern was etched on the 0.020 inch copper face. The conductor pattern supplied the necessary conductors to carry the current to the heating elements as well as the conductors necessary to determine the potential

difference between the guard sections of each heating element. The conductors were of sufficient length so that when the completed heating element section was in place in the tunnel, the conductors would protrude through the base of the working section to facilitate the necessary electrical connections. Plate (1) shows the etched conductor pattern employed. Connections between the conductors on one side of the glass base material and the heating elements on the other side were obtained by plating copper through holes drilled in the base material.

Two such laminates were fabricated, one a mirror image of the other. The two laminates were then cemented together with an insulating material placed between them at the conductor face to form a fin section $1/8$ inch thick. The ends of each element on the same level on each face were joined by drilling through the $1/8$ inch thick section and soldering a pin in place (refer to Figure 2, connection ED).

Plate (2) shows the completed fin heating element section. The heating element grid pattern is plainly visible as are the conductor strips which show through the translucent glass base material.

After etching and cementing together of the two mirror image laminates, the heating element surfaces exposed to the fluid flow were made aerodynamically

smooth. This was accomplished by filling in the regions of the copper grid where copper had been removed by etching with a clear acrylic plastic compound. The resulting surface was completely free of any indentations between the copper grids.

The fin heating element section was bevelled on one edge and notched on the other so that it would be held firmly in place by leading and trailing sections of plexiglass fin material when installed in the tunnel as the central fin in the fin system under study.

Calibration

Two separate calibrations were necessary for each of the eight heating elements. The first, to determine the resistance temperature characteristic of the element and the second to determine the heat transfer area to be used in the calculation of the film coefficient plus a factor to overcome unavoidable heat losses. Each method shall be dealt with in the following paragraphs. The first will be referred to as the "resistance-temperature" calibration and the second as the "flat-plate" calibration.

a) Resistance-temperature calibration

The use of equation (20) in the determination of the heating element resistance variation with temperature depends on the use of known values of R_0 (the element

resistance at a chosen reference temperature) and " α " the temperature coefficient of the material.

$$R_t = R_o (1 + \alpha t) \quad \text{..... (20)}$$

As a result of the small cross-sectional area of the heating element (0.0015 x 0.015 inches) and the effect of any impurity in a conductor of this size it was decided that handbook values for the necessary constants could not be employed.

The heating elements were calibrated by immersing the fin section containing them in a variable temperature oil bath. The bath was allowed to stabilize at a certain temperature. The bath temperature was then read from a standard calibrated thermometer and this value taken as the element temperature. Sufficient time was allowed for the fin section to reach the bath temperature throughout its thickness. A very small current of 0.005 amps, (to minimize any possible heating effect) was passed through the heating element. Values of the current through, and the potential drop across, the active section of each heating element were read from a laboratory standard potentiometer. The heating element resistance was then calculated by use of equation (19). Current values were obtained from the potential drop across an accurately known ~~shunt~~ resistance and the potential values by measuring directly across the active section between the guard sections of each element.

The procedure was repeated so that twenty resistance and temperature values were obtained for temperatures over the range 20°C to 100 °C. Values of element temperature were then plotted against element resistance for each of the eight heating element active sections. From the slopes of these curves and known values of resistance at certain temperatures the values of R_0 , element resistance at 0°C and " α " the temperature coefficient were obtained. Table I lists these values for each of the eight heating elements.

TABLE I
TEMPERATURE COEFFICIENTS AND RESISTANCE
AT REFERENCE TEMPERATURE
FOR HEATING ELEMENTS

Element No.	Resistance at 0° Centigrade " R_0 " ohms	Temperature Coefficient " α " deg C ⁻¹
1	0.2165	4.245×10^{-3}
2	0.2241	4.150×10^{-3}
3	0.2167	4.174×10^{-3}
4	0.2064	4.166×10^{-3}
5	0.1988	4.160×10^{-3}
6	0.1864	4.140×10^{-3}
7	0.1782	4.161×10^{-3}
8	0.1800	4.007×10^{-3}

b) Flat-plate calibration

The calculation of the film coefficient by use of equation (18), assumes accurately known values of surface or heat transfer area and temperature difference between heating element and the fluid stream.

$$h = K E I \quad \dots\dots\dots (18)$$

where $K = \frac{1}{A_s (T_e - T_s)}$

A constant temperature difference may be maintained by element control, but the choice of the heating element area presents some difficulty. To obtain a reasonable element resistance a grid pattern for the heating conductor was used. The surface area of the conductor proper could not be used in equation (17) as the conductor not only supplied heat to the stream from its surface, but it also supplied heat to the spaces between the grids and hence to the stream. The same reasoning applies to the area of the spaces between individual elements. As heat is being removed from these spaces and is supplied by the conductors a temperature profile will then exist across them. Thus if the heating element surface area were considered as the total area between its boundaries plus one half of the area between the elements on each side, the full temperature difference could not be taken as

acting on this area. It was not considered convenient to modify the temperature difference term hence the area term had to be corrected.

A mathematical solution for this correction by a method of relaxation was tried but it was considered that direct calibration against an existing proven theory should be carried out.

A further complication with the elements was observed during the initial trial runs. Heat losses through the potential section conductors were detected. Heat was applied to these conductors in an attempt to eliminate the loss but this was unsuccessful. The potential conductors were shortened at the fin as may be seen by comparing Plates (1) and (2), also the leads from the fin to the control panel were reduced in size. The loss, though smaller, still persisted. As this heat loss would be constant if the heating element temperature was maintained constant and the correction to be applied to the area would be a function of the fluid velocity, the correction factor including both these points would vary with fluid velocity. The effect of the loss through the conductors would be much more pronounced at the lower fluid velocities.

Equation (22) suggested a method of calibration. If the velocity were held constant over the face of the fin, the film coefficient could be

predicted by equation (22). The film coefficient could also be calculated from experimental values by equation (18). A factor which would modify the results of equation (18) to agree with equation (22) could then be calculated.

$$\frac{h_{\text{theoretical}}}{h_{\text{experimental}}} = \text{Correction Factor} \quad \dots\dots (24)$$

The above method of calibration was used. The fin containing the heating elements was set up along the center-line of the tunnel as a flat plate. A boundary layer control system was developed to remove the boundary layer from the bottom of the tunnel by suction. Constant fluid velocity from fin tip to fin root on both sides of the fin was obtained. Plate (3) shows the boundary layer control slots in the tunnel base and Plate (4) shows the working section of the tunnel during this flat plate calibration.

The fluid velocity over the flat plate was varied over a range of 20 to 150 feet per second. Film coefficients were obtained experimentally and correction factors calculated. Element number one at the top of the fin and element number eight at the bottom were not used as active elements as they acted as guard elements for the remaining six elements between them. Table II gives the correction factors for the active elements for the case of fluid velocity equal

to 100 feet per second.

TABLE II
ELEMENT CORRECTION FACTORS FOR AREA AND
HEAT LOSSES
VELOCITY OF 100 f.p.s.

Element No.	Correction Factor
2	0.7525
3	0.9180
4	1.1050
5	0.9000
6	0.8060
7	0.7600

Control of Elements

Precise control over each of the heating elements which make up the heat transfer fin is essential if the fin section is to be maintained isothermal. In order to be controlled individually each heating element had to operate on its own circuit. Two prime variables had to be measured accurately without affecting the element circuit. These variables were the potential drop across the active section of the element and the current through it. The ratio of these two variables indicates the element temperature and their product is a measure of the film coefficient.

Direct visual indication of the element resistance (hence temperature) was required if stable operating conditions were to be arrived at in the shortest possible time with the least amount of difficulty. This was accomplished by having the element form one arm of a Wheatstone resistance bridge. A zero centering galvanometer would indicate whether the element temperature was too high or too low as well as indicate when the bridge was in balance. By suitable choice of the resistance values for the arms of the bridge this null balance could be made to occur at the desired element temperature. Figure 3 shows the bridge circuit employed for each of the eight elements.

A steady direct current voltage was supplied to bridges through the use of two high load capacity 6 volt storage cells. The storage cells were arranged so that they could supply either 6 or 12 volts to the eight bridge circuits. The voltage supplied to each individual bridge and hence the current through the heating element was controlled by two rheostats in series, one for coarse control and the other for fine control. The resistance designated as " R_c " in Figure 3 was variable and could be pre-set to balance the bridge at the desired temperature. The galvanometer reading served only as an indication of the temperature and temperature values as calculated by the use of

equation (21) were used for final current adjustment and film coefficient calculations.

The potential drop across the active section of each heating element was read from a direct reading self balancing, 0 to 10 millivolt Leeds and Northrup potentiometer. The potentiometer could be connected to any one of the eight elements through a multi-point switch. A voltage divider was used so that the drop across the active section of the element would agree with the potentiometer input requirements.

The current through the element was measured as a potential drop across a 0.00512 ohm shunt, placed in the arm of the bridge containing the heating element. A 20 point Brown, self balancing, direct reading 0 to 20 millivolt potentiometer was used for this purpose.

Plate (5) shows the control panel with the temperature setting resistances, the coarse and fine current controls, the zero centering galvanometer and the two potentiometers used.

Auxiliary circuits included a charging facility for the storage batteries, a series-parallel switching arrangement for 6 or 12 volt bridge supply and in interlocking circuit between the 550 volt, 3 phase fan supply and the element power supply. This interlocking circuit was considered necessary as

should the fans stop and the flow of air over the heating elements decrease, the currents through the elements would burn them out.

PROCEDURE AND RANGE OF TESTS

The test procedure used is as follows. All tests were run with a heating element temperature of 50°C. A fin spacing was chosen and the fin system placed in the working section of the tunnel. The flow control was adjusted to give maximum free stream velocity in the working section. The current through each of the eight heating elements was adjusted until all elements reached the required temperature. The current and potential drop for each element were then recorded. At the same time the entire flow field velocity pattern between the fins was obtained by the traverse mechanism.

Tests were run in the same manner for the cases of $3/4$, $1/2$ and $1/4$ maximum velocity with the fin system under investigation. On the completion of the test series with one spacing, the fin system was removed from the tunnel, the spacing changed and the above test procedure repeated.

Tests were run with fin spacings of $3/8$, $1/2$, $5/8$ and $3/4$ inches and constant fin height of $1\ 1/2$ inches. These spacings correspond to fin height to spacing ratios of 4.0, 3.0, 2.4 and 2 respectively. The velocities covered corresponded to a range of Reynolds' Numbers of 1.85×10^5 to 1.43×10^6 based on the distance from the hydrodynamic leading edge.

RESULTS AND DISCUSSION

Experimental values of the film coefficient "h" were obtained through the use of equations (18), (22) and (24). These values are shown plotted for the cases of 3/8, 1/2, 5/8 and 3/4 inch fin spacings versus the velocity at the centerline of the fin flow channel in Figures 5, 6, 7 and 8 respectively.

The curve which best suited the experimental values was obtained using a "Forsythe"¹¹ curve fitting routine on an I.B.M. 650 digital computer. This routine fits a curve to the data points by a method of least squares using orthogonal polynomials. From the generally accepted form of the Nusselt equation:

$$N_{Nu} = A N_{Re}^a N_{Pr}^c \quad \dots\dots\dots (25)$$

and visual indication of the plotted experimental results a relation of the form;

$$h = A_0 V^a \quad \dots\dots\dots (26)$$

was assumed to fit the data. Equation (26) is valid in this form as all the variables other than the film coefficient "h" and the velocity "V" making up the non-dimensional groupings in equation (25) were held constant during the tests. Equation (26) was written in logarithmic form,

$$\ln h = \ln A_0 + a \ln V \quad \dots\dots\dots (27)$$

and presented to the computer as a polynomial of the first order. Values of $\ln A_0$ and a were obtained directly from the computer results. Table III gives the values of A_0 and a to be used in equation (26) for the various fin spacings under investigation.

TABLE III

Fin Spacing	"A" 0	"a"
3/8"	0.3839	0.89
1/2"	0.5865	0.82
5/8"	0.5040	0.82
3/4"	0.4061	0.84

As previously mentioned, the values of the constants for use in equation (26) were obtained from results with a fixed temperature difference, hence constant values for fluid viscosity, thermal conductivity, density and specific heat. Expressing the results in the non-dimensional grouping form of equation (25) and using the accepted value of $1/3$ for the exponent " c " in the Prandtl number, we have the constants " A " and a as shown in Table IV.

Inspection of table IV reveals the following indications, firstly that the value of the exponent " a " is relatively constant over the range of

TABLE IV

Fin Spacing	A	a
3/8	0.0135	0.89
1/2	0.0390	0.82
5/8	0.0335	0.82
3/4	0.0223	0.84

fin spacings, and secondly, that the value of the constant "A" to be used in equation (25) varies with fin spacing. This variation in constant "A" is such that the film coefficient appears to increase with decreasing fin spacing to some value then decrease again. The increase is noted between spacings of 3/4, 5/8 and 1/2 inch, while a decrease is noted between 1/2 and 3/8 inch spacings.

The values as tabulated in Table IV for the fin spacing of 3/8 inch require some further explanation. No mention has been made of probable error. The probable error in the calculation of the film coefficient based on the maximum possible error in the measured values is of the order of 10%. The effect of this error on the constant "A" and the exponent "a" is estimated at 5%. If this error were applied to the exponent "a" for the case of the 3/8 inch spacing to bring the exponent more into line with the exponents of the other spacings, then for the same Nusselt number obtained

through the use of equation (25), the value of the constant "A" would increase to some extent. Even this increase, however, would still leave the value of constant "A" for the $3/8$ in. spacing well below that for $1/2$ in. spacing. Thus even when considering the effect of errors resulting from experimental apparatus and procedure, the results suggest a film coefficient which increases to some optimum value with decreasing fin spacing, then decreases with a further decrease in fin spacing. As the series of tests were conducted with a constant fin height, it is possible that the constant "A" is some function of the fin height to spacing ratio.

Present results are not sufficient to evaluate a mathematical relationship but a possible explanation of the variation in film coefficient with fin spacing may be attempted by considering the flow pattern in the rectangular flow channel between successive fins. Boundary layers exist not only on the fin surfaces but also at the base of the rectangular flow channel. Considering the corner of the rectangular flow channel we have boundary layers in two planes intersecting each other at right angles, as shown by Figure 9. The result of this intersection is to produce secondary flows in the rectangular flow channel. A typical secondary flow pattern is shown in Figure 10. These

secondary flows produce velocities in the corner region which are higher than would be expected for a normal boundary layer velocity distribution. Nikuradse¹², through experimental investigation of flow in non-circular ducts was first to notice these high velocity regions and explained them as due to vortices forming in the corners. Prandtl¹³ reasoned that they were formed by a momentum transfer between regions of high and low shearing stress, but the ultimate physical cause of this secondary flow has yet to be established.

Figure 11 shows velocity profiles for a typical fin height to spacing ratio obtained in the present tests. The effect of the secondary flow vortices on the velocity distribution is plainly visible and is more pronounced in the region near the bottom of the flow channel. As the spacing is decreased the effect of the secondary flow is to extend the high velocity region deeper into the flow channel, which results in higher values of the film coefficient. If the spacing is further decreased it is possible that the secondary flow vortices inter-react with each other to such an extent that they partially cancel and are no longer able to propagate the higher velocity of the free stream above the flow channel down into the flow channel. The result is lower velocities in the flow channel near the fin surfaces and correspondingly lower film coefficients. Thus with the preceding

explanation it is possible to imagine an optimum fin height-to-spacing ratio.

The existence of an optimum was recognized by Schmidt¹⁴, and Wagener¹⁵. Schmidt suggested that the spacing should not be less than two fin surface boundary layer thicknesses at the fin exit. Wagener suggested a value some 12% greater than Schmidt. Both the above cases suggest that it was not fully realized that the secondary flow effects could be used to advantage. In both cases the spacing would be such that the flow would not be fully developed.

Schey and Ellerberock¹⁶, working with fins on a cylinder show increasing film coefficients with spacings increasing from 0.02 to 0.20 inches. The case of flow through fin channels around a cylinder is not directly analogous to longitudinal flow but nevertheless it supports the reasoning that film coefficients are not only a function of velocity but also fin spacing.

The case of the flat plate with a turbulent boundary layer was studied by Johnson and Rubesin¹⁷, the relation for the average Nusselt number being given as follows:

$$\bar{N}_{Nu_x} = 0.037 N_{Re_x}^{0.8} N_{Pr}^{1/3} \dots\dots\dots (28)$$

This relation is obtained from integrating local values as given by;

$$N_{Nu_x} = 0.0288 N_{Re_x}^{0.8} N_{Pr}^{1/3} \dots\dots\dots (29)$$

Comparison of equation (29) and of equation (25) with the appropriate constants for the various fin spacings indicates that there is a definite similarity between the case of film coefficients calculated by flat plate relations and those calculated by a similar relation suitably modified for fin height to spacing ratio. The Reynolds number in the first case is based on the velocity of the free stream over the flat plate and in the second case is based on the velocity in the flow channel between two successive fins.

Local coefficients calculated using equation (14) resulting from the work of Ghai⁶ predict a much larger decrease in coefficient value from fin tip to fin root than was actually experienced. Direct comparison is not possible, as Ghai's correlation is not based on local values of velocity but on the velocity at the entrance to the fin system. The larger predicted decrease is understandable, as with the range of velocities and spacings employed by Ghai the flow in the region where the film coefficient was experimentally determined was not at all times fully developed. It is also interesting to note that Ghai's correlation as given in equation (14) makes no provision for the possibility of an optimum fin height to spacing

ratio, but for all fin height to spacing ratios the maximum film coefficient occurs at the fin tip and has a value equal to that predicted by flat plate theory.

Since very little work has been done in this particular phase of the heat transfer field, there is no previous work against which the results of the series of tests carried out may be compared directly.

CONCLUSIONS AND RECOMMENDATIONS

From the results of the tests carried out it is concluded that film coefficients on the surface of longitudinal fins may be predicted by relations similar to those used for predicting film coefficients with flow over a flat plate, provided the velocity distribution within the flow channel between the fins is known. The results strongly suggest that the film coefficient is not only a function of the fluid velocity but also of the geometry of the fin system under consideration. This is evident from the variation of the film coefficient with the geometric parameter of the fin height-to-spacing ratio. It is further suggested that some optimum condition, which depends on the geometric configuration, exists.

It is obvious that in order to obtain average film coefficients for use in heat exchanger design, a complete knowledge of the local values is required. Furthermore, correlations of local values based on inlet velocity are of limited use as with most fin systems the inlet velocity is not the same as the free stream velocity above the rectangular fin flow channel. The free stream velocity above the fins changes with position down the fin length, and is obviously some function of the inlet velocity to the

fin system, the geometric configuration of the fins and the geometry of the duct which contains the fins. Similarly the velocity distribution within the fin channels bears a definite relation to the fin spacing and to the free stream velocity above the fins. Thus a successful correlation, based on a representative average velocity at inlet, or elsewhere, cannot be developed until the above mentioned factors have been studied and until their effect on flow behaviour within passages containing fins be predicted.

The work reported in this thesis has only scratched the surface of the general problem but at the same time it has served to indicate what factors are involved, their relative importance and a possible approach to a complete solution. As a result of these facts it is strongly recommended that more research be carried out in the direction indicated by this investigation.

It is recommended that a new film coefficient transducer which does not require such a delicate calibration and which possesses an accuracy of the order of $\pm 1\%$ be developed. This is considered necessary as the results indicate that the film coefficients do not change by the extent that previous correlations predicted and it was on these predictions

*that the present heating-element system was designed.

It is possible that the required accuracy may be achieved by adapting a commercially available heat-flow transducer to the requirements of this problem.

REFERENCES

1. Lemmon Jr., A.W., Colburn, A.P., and Nottage, H.B.
"Heat Transfer from a Baffled Cylinder to Air"
Trans. Am. Soc. Mech. Engrs., Vol. 67, p. 601, 1945.
2. McAdams, W.H., Drexel, T.B., and Goldey, R.H.,
"Coefficients for Heat Transfer around Finned Cylinders"
Trans. Am. Soc. Mech. Engrs., Vol. 67, p. 613, 1945.
3. Harper, W.P. and Brown, D.R.
"Mathematical Equations for Heat Conduction in the
Fins of Air Cooled Engines"
N.A.C.A. Rept. 158, 1922.
4. Gardner, K.A.
"Efficiency of Extended Surfaces"
Trans. Am. Soc. Mech. Engrs., Vol. 67, pp. 621-631,
1945.
5. Ghai, M.L. and Jakob, M.
"Local Coefficients of Heat Transfer on Fins"
Am. Soc. Mech. Engrs., Paper no. 50-S-18, 1950.
6. Ghai, M.L.
"Local Coefficients of Heat Transfer on Straight Fins"
Illinois Institute of Technology,
Ph.D. Thesis, 1949.
7. Scesa, S.
"Experimental Investigation of Convective Heat Transfer
to Air From a Flat Plate with a Stepwise Discontinuous
Surface Temperature"
University of California, M.S. Thesis, 1949.
8. Rubesin, M.W.
"An Analytical Investigation of Convective Heat
Transfer from a Flat Plate with a Stepwise Discontinuous
Surface Temperature"
University of California. M.S. Thesis, 1947.

9. Jakob, M. and Dow, W.M.
"Heat Transfer from a Cylindrical Surface to Air in Parallel Flow with and without Unheated Starting Sections"
Trans. Am. Soc. Mech. Engrs., Vol. 68, p. 123, 1946.
10. Beauregard, J.P.
"The Mixing of Cold Air Jets with a Hot Gas Stream"
McGill University, M. Eng. Thesis, 1952.
11. Forsythe, G.E.
"The Generation and Use of Orthogonal Polynomials for Data Fitting with a Digital Computer"
University of Toronto, S.I.A.M. Vol. 5, No. 2, 1957.
12. Nikuradse, J.
"Untersuchung über die Geschwindigkeitsverteilung in Turbulenten Strömungen"
Forschungsarbeiten des Ver Deutsch Ing.
No. 281, 1926.
13. Prandtl, L.
"Elementary Fluid Dynamics"
Academic Press.
14. Schmidt, E.
"Die Wärmeübertragung Durch Rippen"
Zeitsch. Ver. Deutsch Ing. No. 70, 1926.
15. Wagener, G.
"Der Wärmeübertragung an Kühlrippen"
Beiheft zum Gesundheits Ingenieur
Reihe 1 Heft 24, 1929.
16. Schey, O.W. and Ellerberock, H.H.
"Blower Cooling of Finned Cylinders"
N.A.C.A. Rept. No. 587, 1937.
17. Rubesin, M.W. and Johnson, H.A.
"Aerodynamic Heating and Convective Heat Transfer"
Am. Soc. Mech. Engrs. Vol. 71, pp. 447-456, 1949.

APPENDIX I

General Apparatus

The basic requirement faced in the design of the test apparatus was a suitable supply of moving air with velocities which could be varied from values of 20 feet per second to 150 feet per second. Preliminary considerations evaluated the possibility of incorporating the necessary heat transfer coefficient apparatus in an existing air supply. It was decided that a small low speed wind tunnel should be designed to meet the specific requirements of the research to be carried out. Plate (6) shows the completed wind tunnel and the general layout employed. The actual tunnel as constructed is best described in terms of its basic components.

The wind tunnel intake was a modified version of that used by J. Beauregard¹⁰ in his research, the profile of which had been calculated on potential flow principles to minimize losses. As the intake had previously been constructed with a balsa wood flow surface on a soft wood frame, modifications to its profile were carried out without difficulty. A contraction ratio of 9:1 was used and the intake was mounted so that it could be moved in the horizontal plane along the tunnel axis to facilitate the removal

of the test section or accept test sections of different lengths. Losses with the intake were negligible and a flat velocity profile over the tunnel operating range was assured. Refer to Figure 4 for a typical profile.

Clear acrylic plastic (plexiglass) was used to construct the working section of tunnel. The material was chosen so that visual verification of velocity probe location could be made, also flow patterns could be observed by the use of a tracer technique should they be required. The bottom of the working section was fitted with one inch thick removable plywood bases into which slots were milled to accept 1/8 inch thick clear acrylic plastic fins. Several bases were made so that fin systems with height of 1 1/2 inches and spacings that varied from 3/8 inch to 3/4 inch could be inserted in the working section. Plate (7) shows a typical fin system. Provision was made so that clear plastic filler strips could be mounted to the top of the tunnel to decrease the head space above the fins in the working section. The centre fin in the working section was machined to accept the film coefficient transducer, previously described. A velocity traverse mechanism capable of traversing the entire area in the flow channel between the fins was fitted to the base. This mechanism is shown in Plate (8).

Diffusion of the flow after the working section was accomplished by a square to round transition

section followed by a 10 degree included angle sheet metal diffuser of sufficient length so that the diffuser diameter equalled that of the flow control.

Flow control, i.e. control of the velocity of the fluid in the working section was obtained by a method of bleeding in air to the constant speed fan suction source. Two cones, one male and the other female were constructed of sheet metal and mounted to the diffuser and suction source respectively. The suction source was free to move between guides along the axis of the tunnel. By moving the suction source backwards or forwards, the amount of bleed through the annular area of the two cones could be controlled and hence the velocity of the fluid in the working section of the tunnel. Flow stability was insured with this method as no matter what tunnel velocity was desired, the fans in the suction source always operated on a stable section of their flow versus pressure characteristic.

The suction pressure required by the tunnel was supplied by a two stage, counter rotating, "Wood Aerofoil", 550V AC, 3 phase, 12 inch diameter fan unit. The unit was mounted so that it was free to move along the tunnel axis for reasons previously mentioned.

A diffuser was attached to the exhaust of the fan unit to remove any possible losses at this point and also to attenuate the noise. Both the flow control and fan unit are shown in Plate (6).

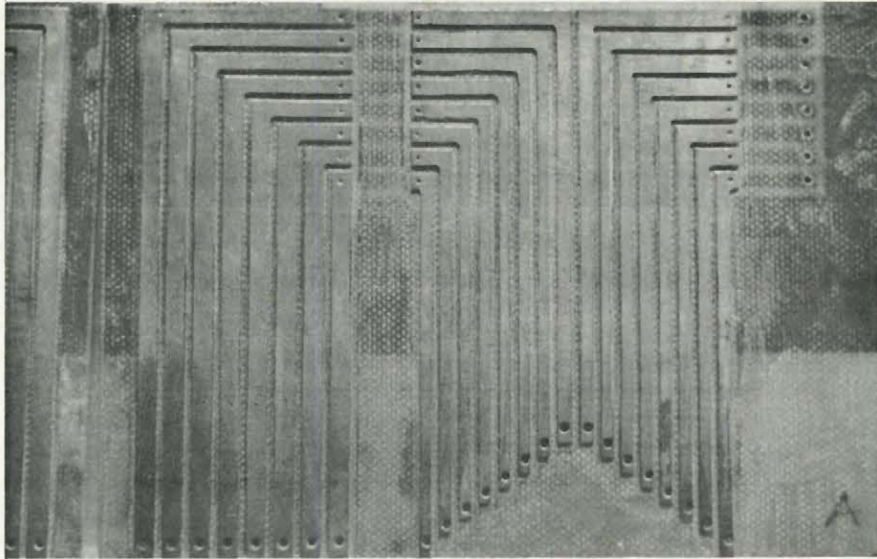


Plate 1
Conductor Pattern

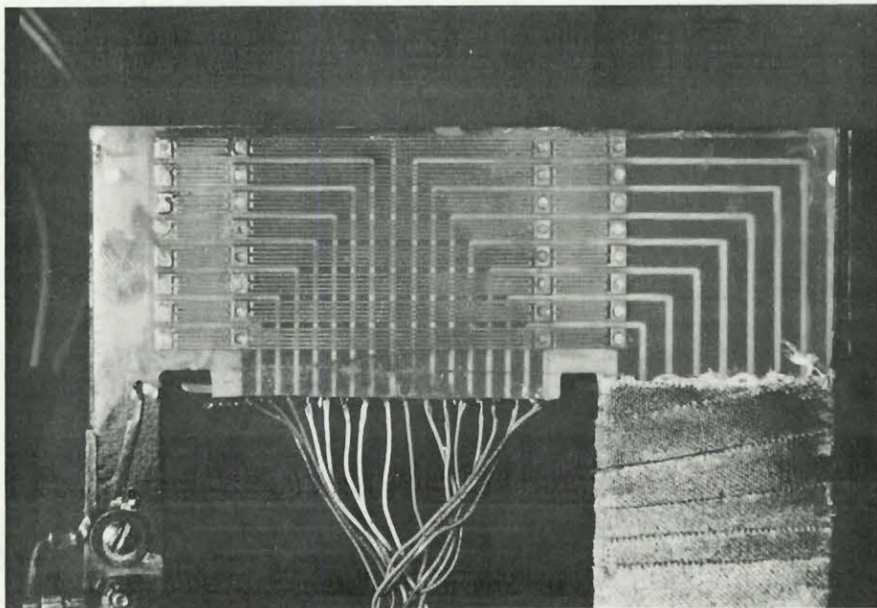


Plate 2
Film Coefficient Transducer

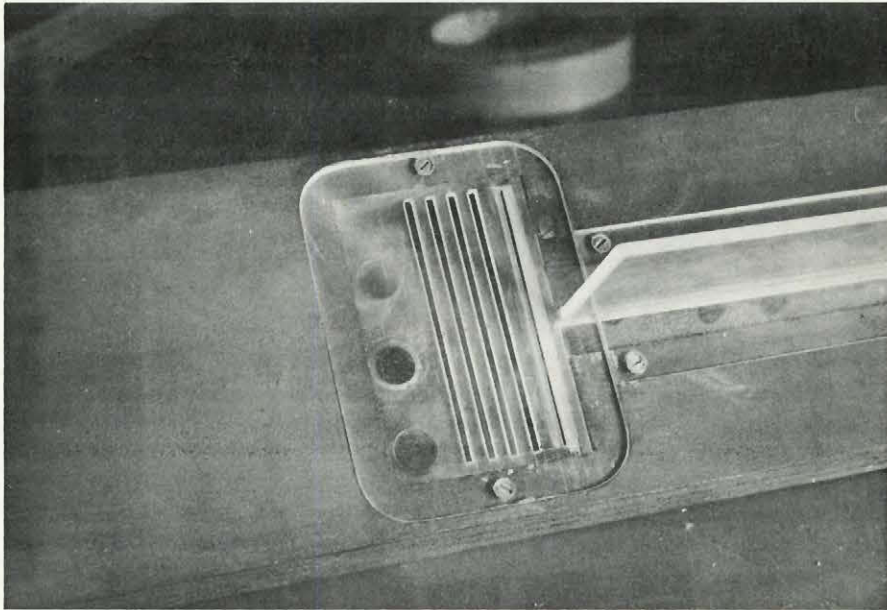


Plate 3
Boundary Control Suction Slots

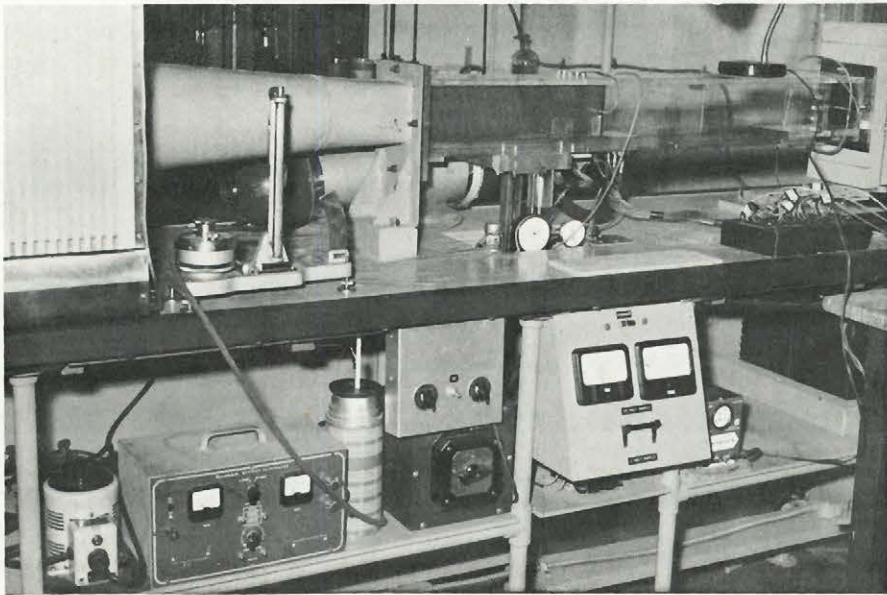


Plate 4
Wind Tunnel Working Section

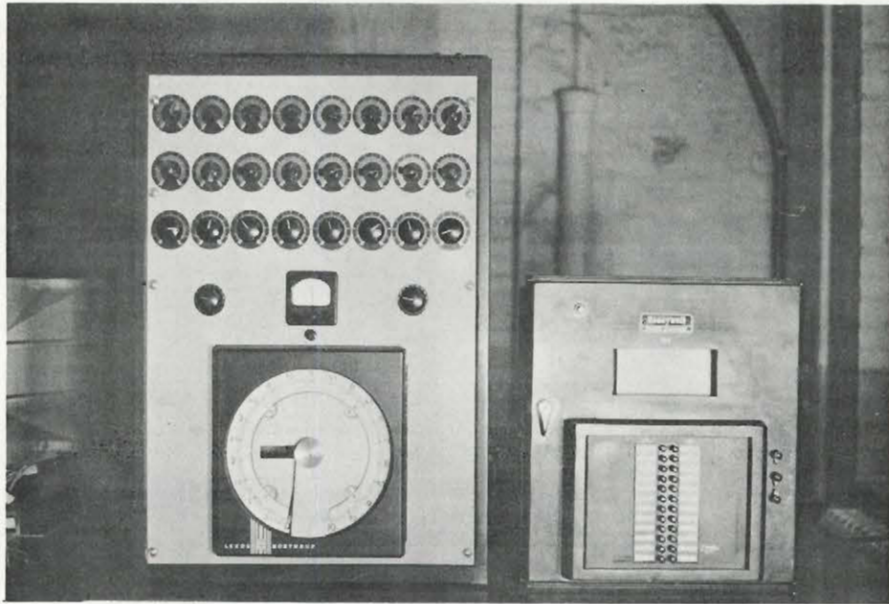


Plate 5
Control Panel

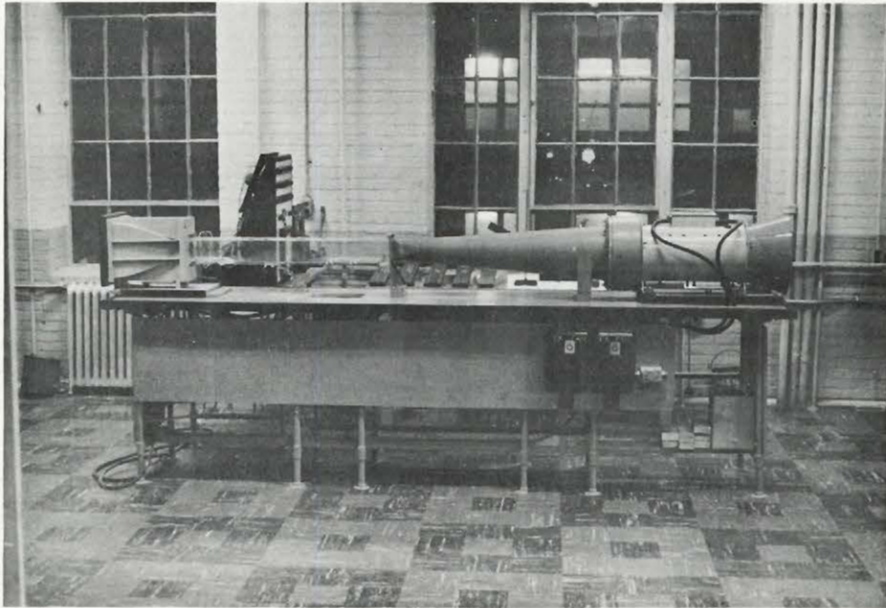


Plate 6
Wind Tunnel

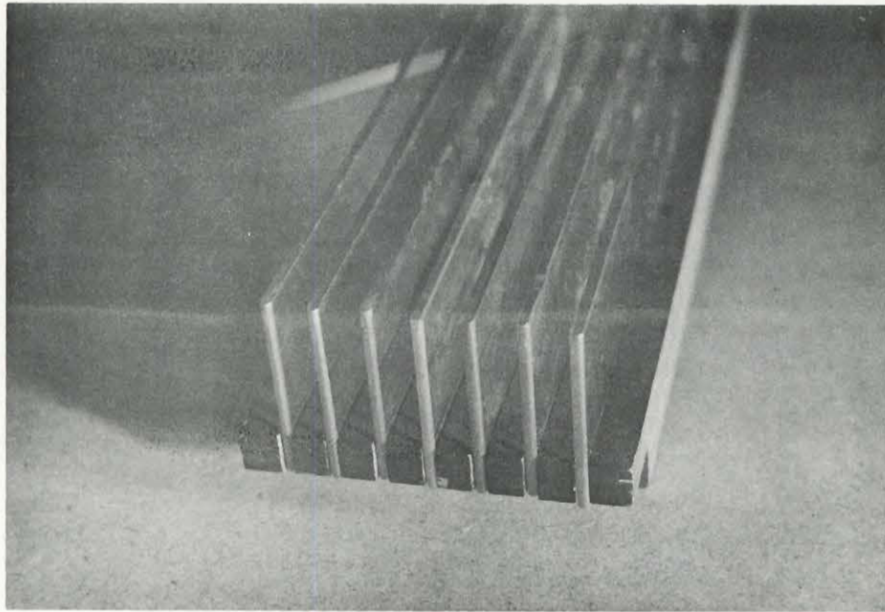


Plate 7
3/8" Spacing Fin System

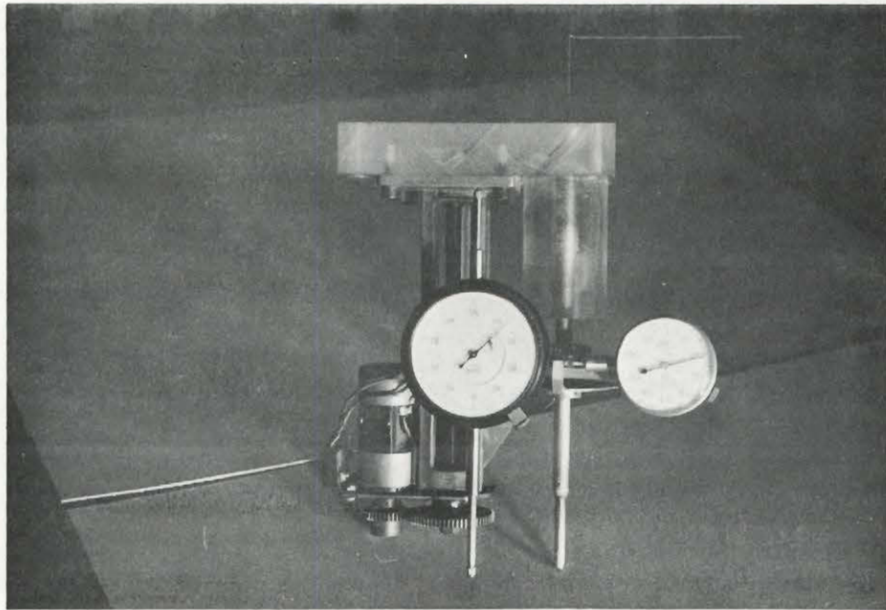


Plate 8
Velocity Traverse Mechanism

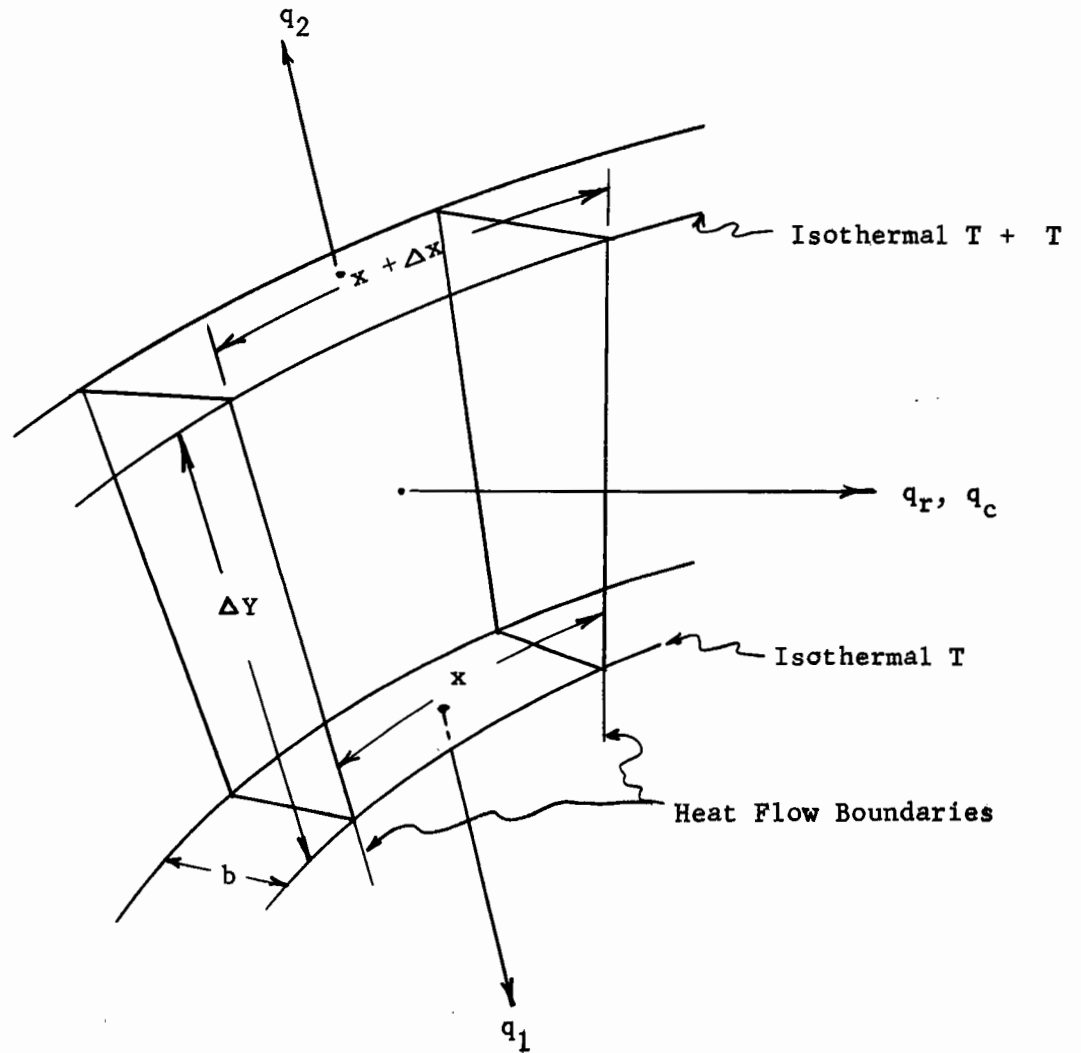
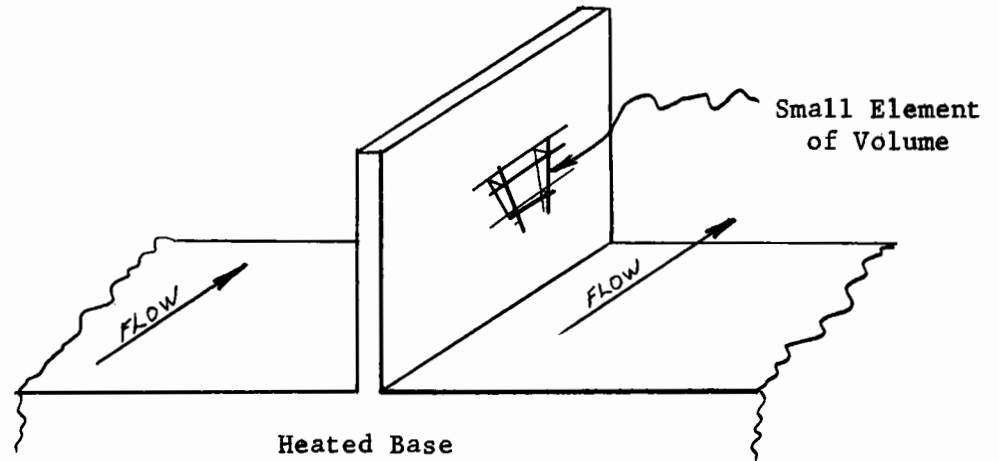


FIGURE (1)

FIN AND SMALL ELEMENT OF VOLUME BOUNDED BY
ISOTHERMALS AND HEAT FLOW BOUNDARIES

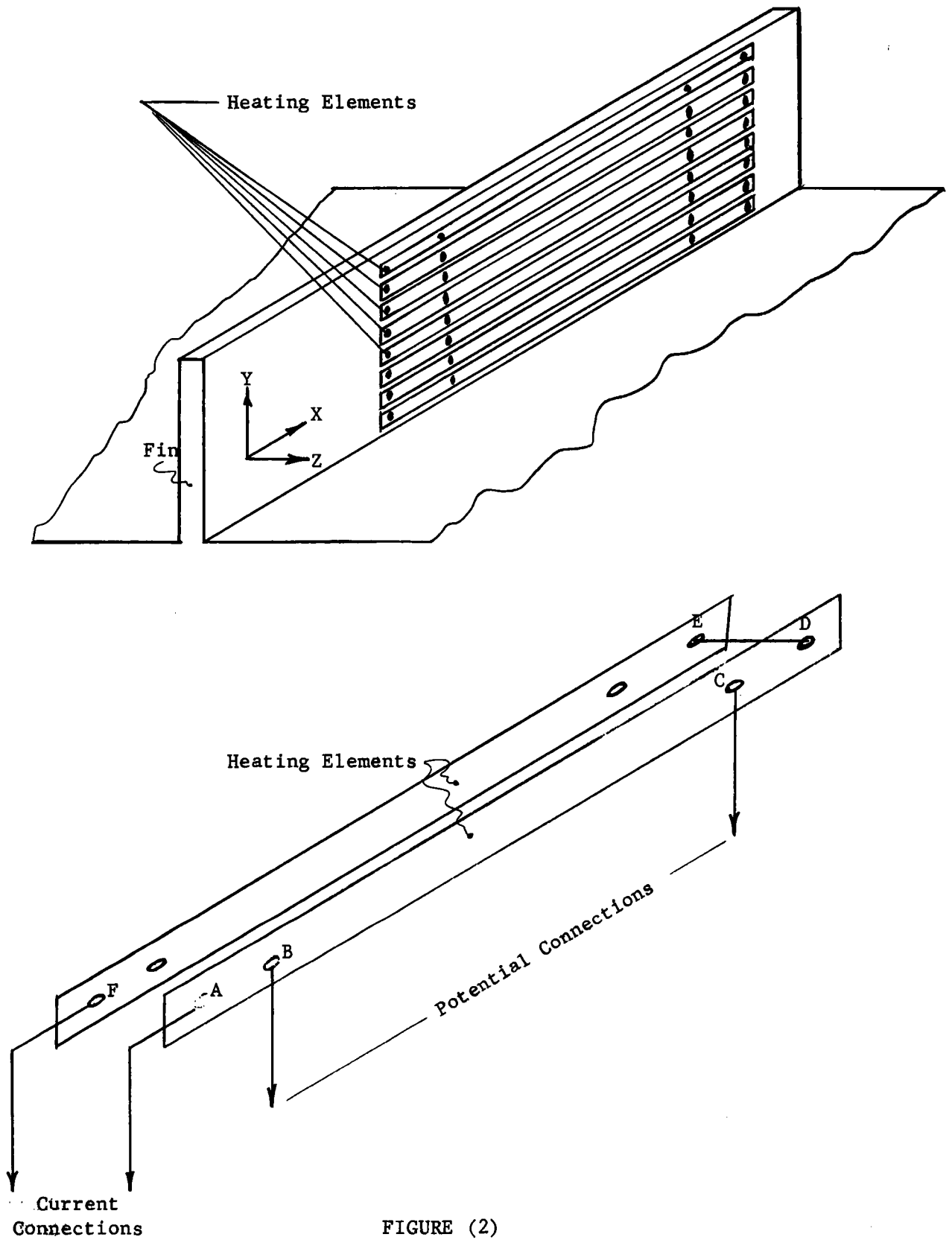


FIGURE (2)
HEAT TRANSFER FIN
AND HEATING ELEMENTS

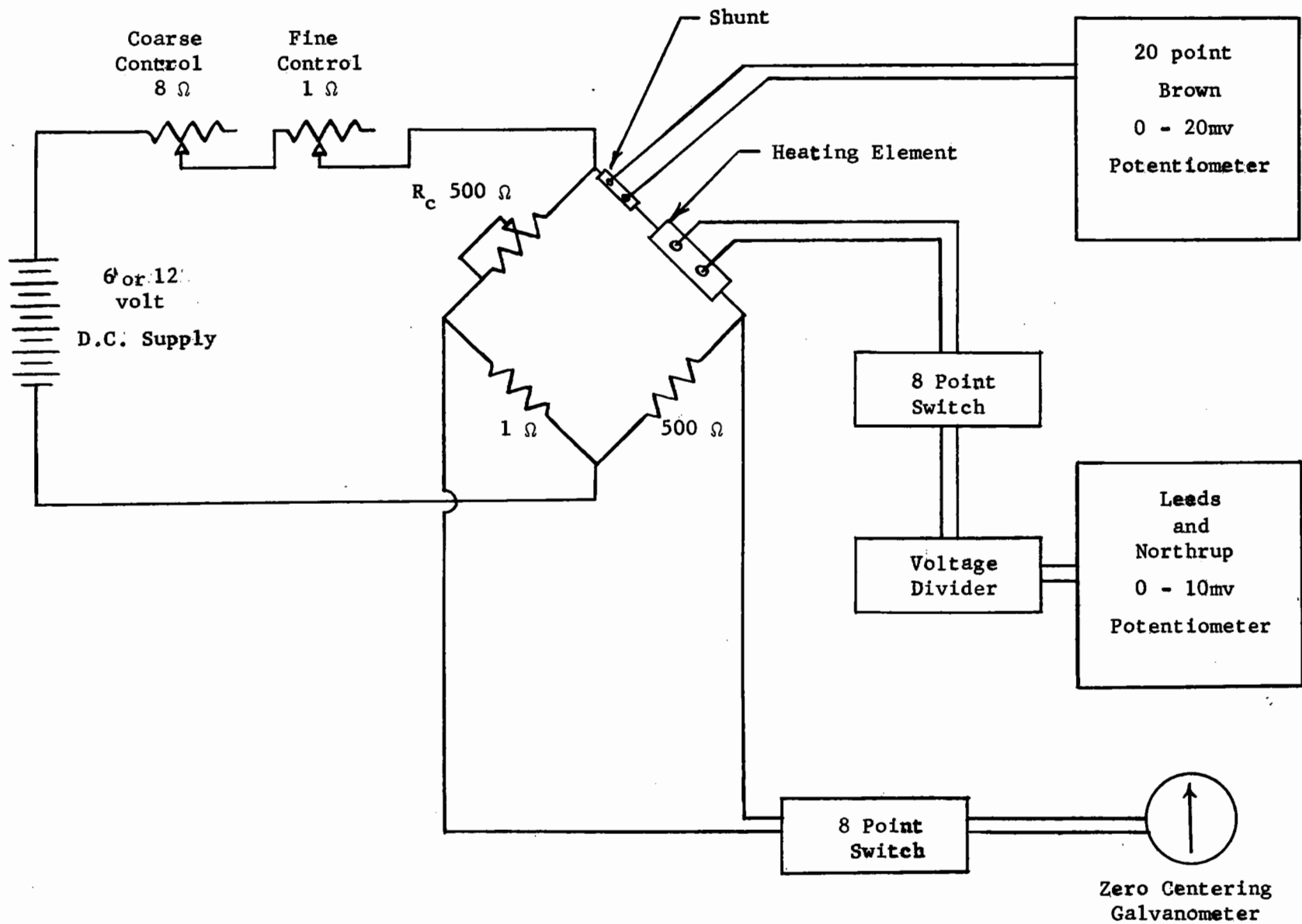
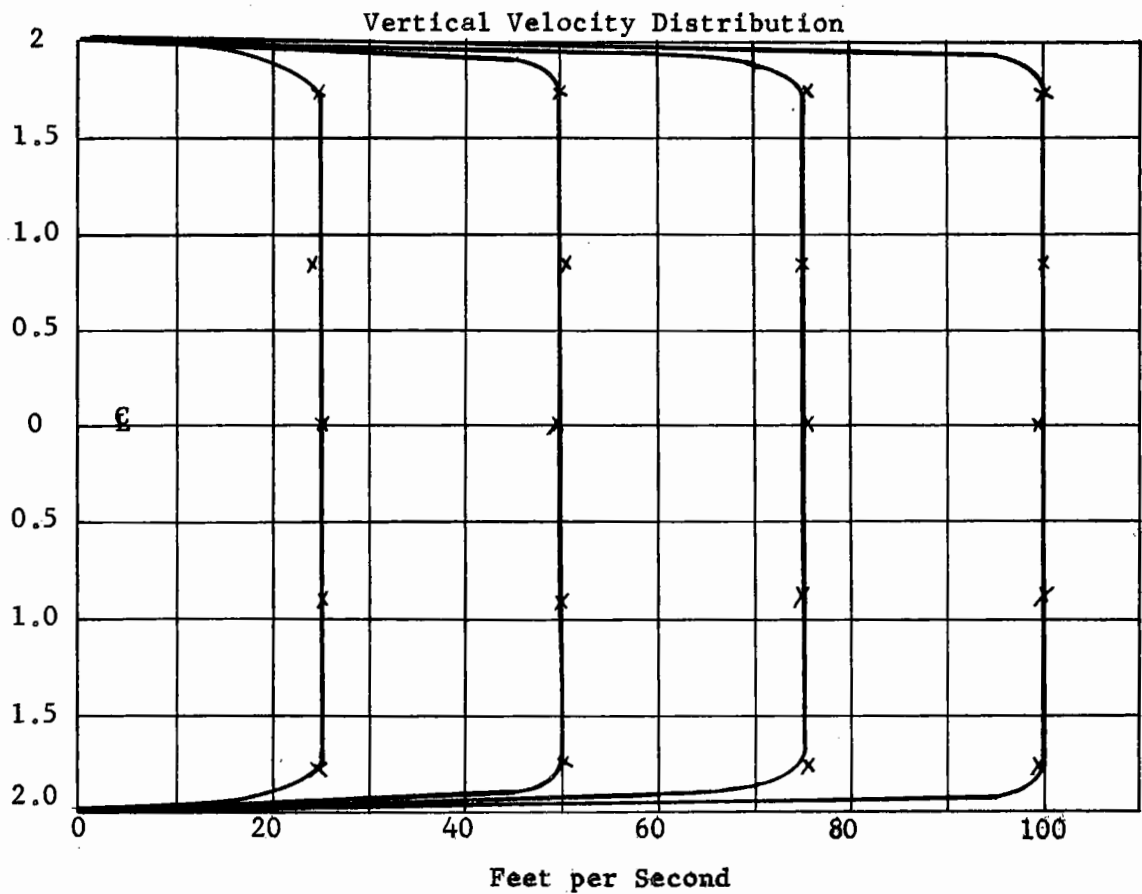
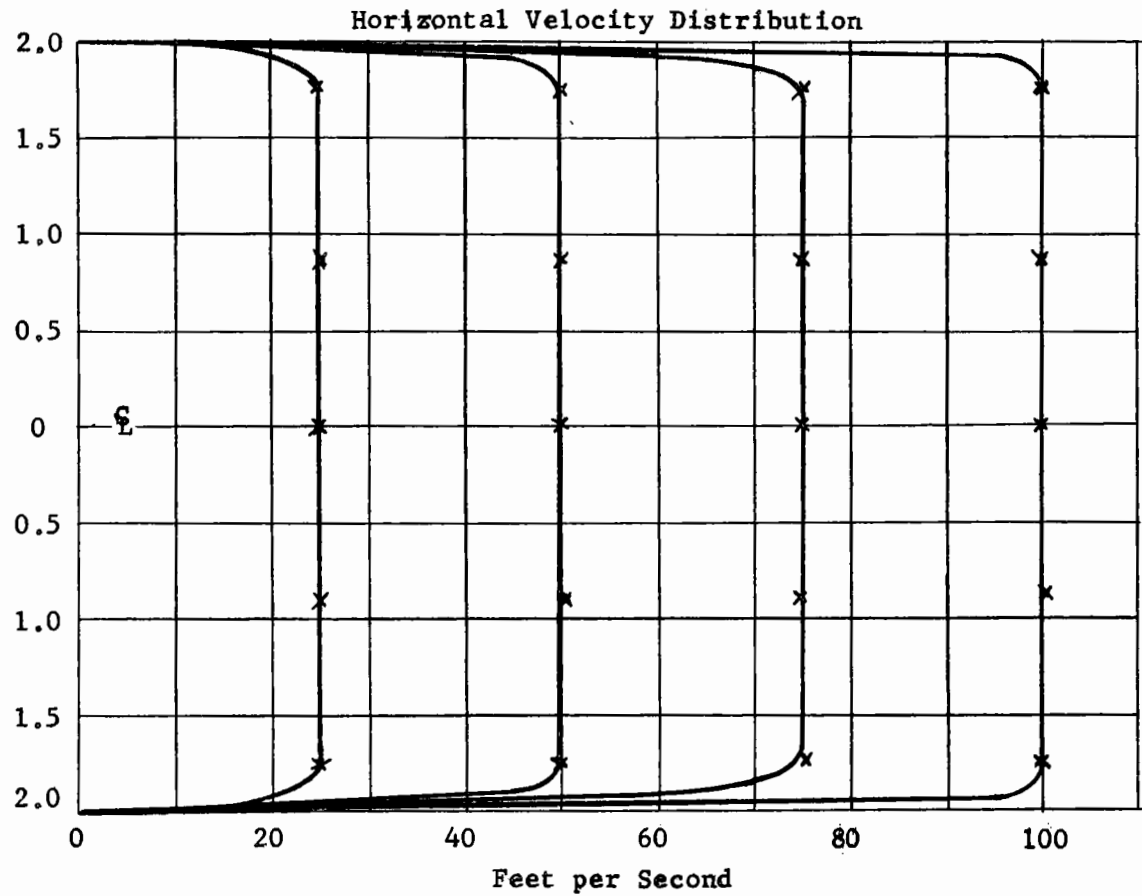


FIGURE (3)

CONTROL AND MEASURING CIRCUITS

FIGURE (4) TYPICAL FLOW PROFILES AT INLET TO FINS



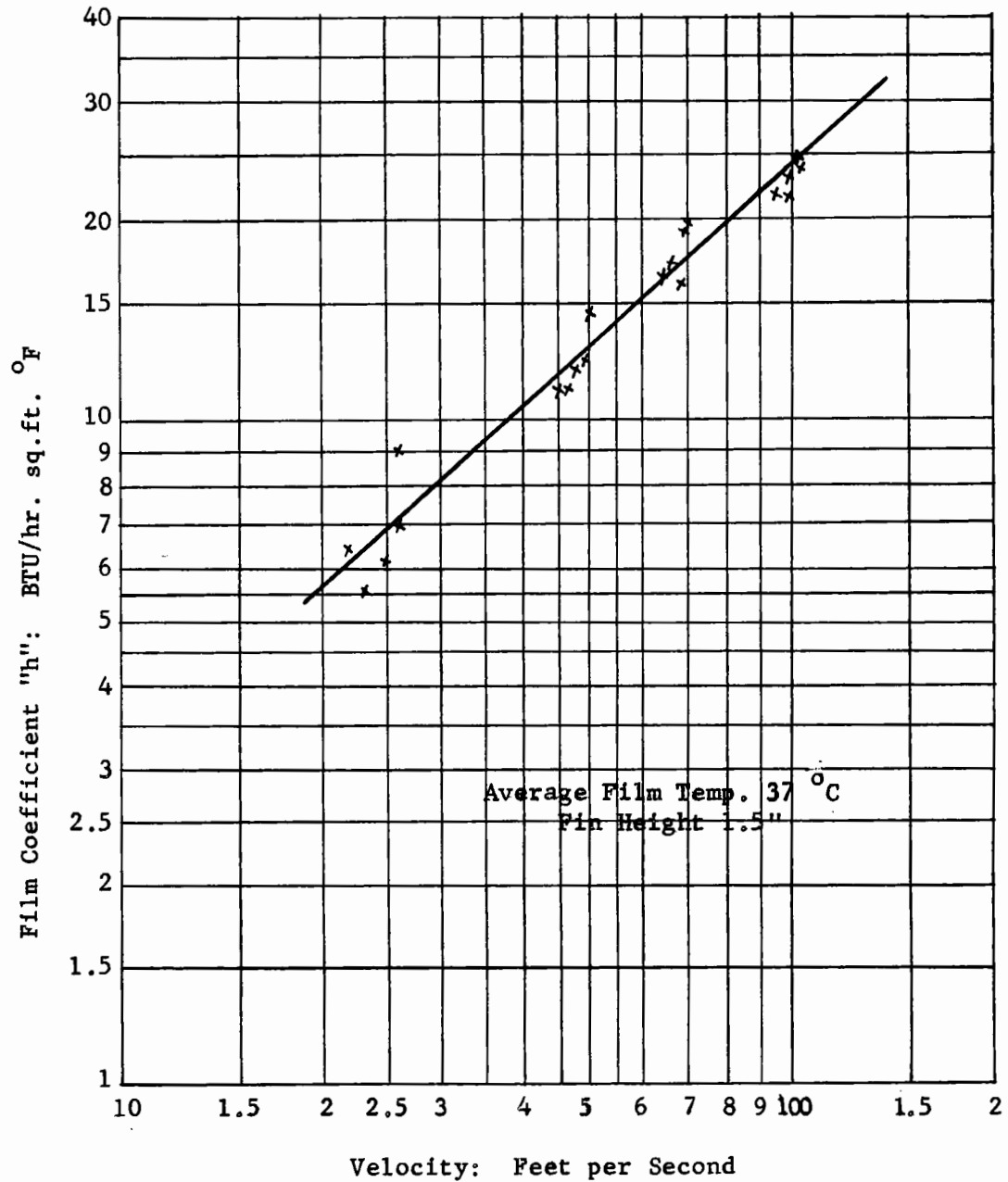


FIGURE (5)

FILM COEFFICIENT VS. VELOCITY

3/8" FIN SPACING

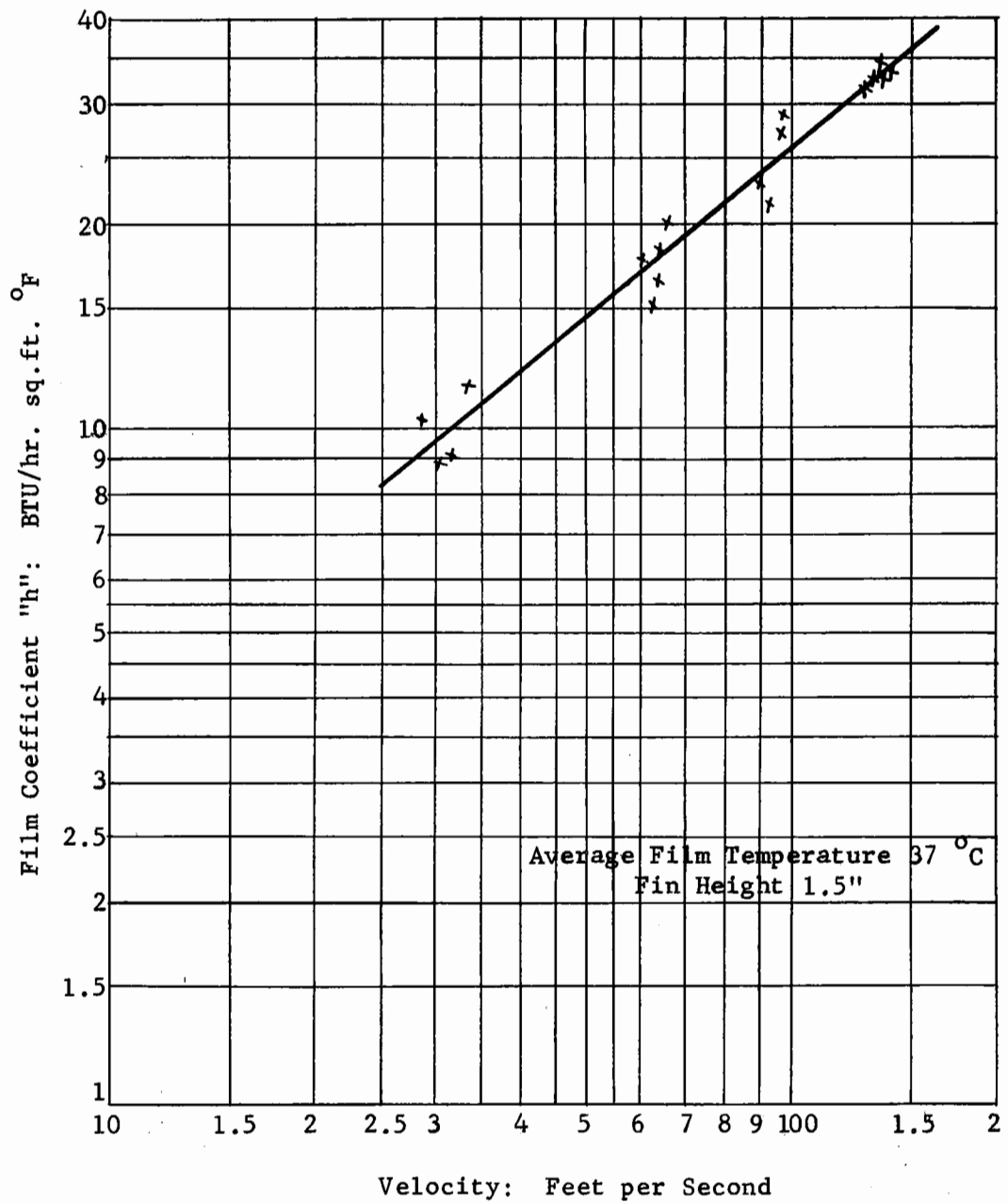


FIGURE (6)

FILM COEFFICIENT VS. VELOCITY

1/2" FIN SPACING

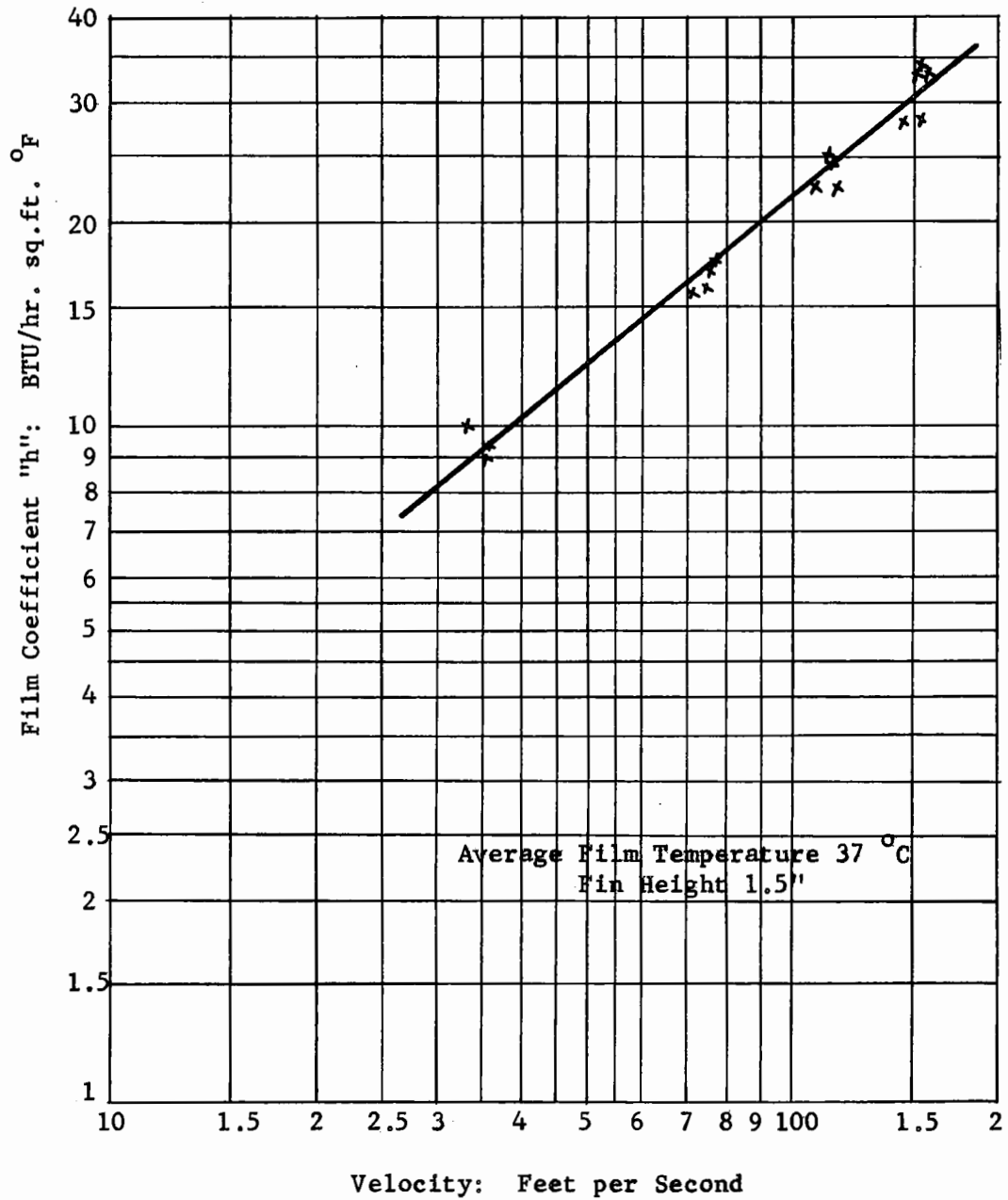


FIGURE (7)

FILM COEFFICIENT VS. VELOCITY

5/8" FIN SPACING

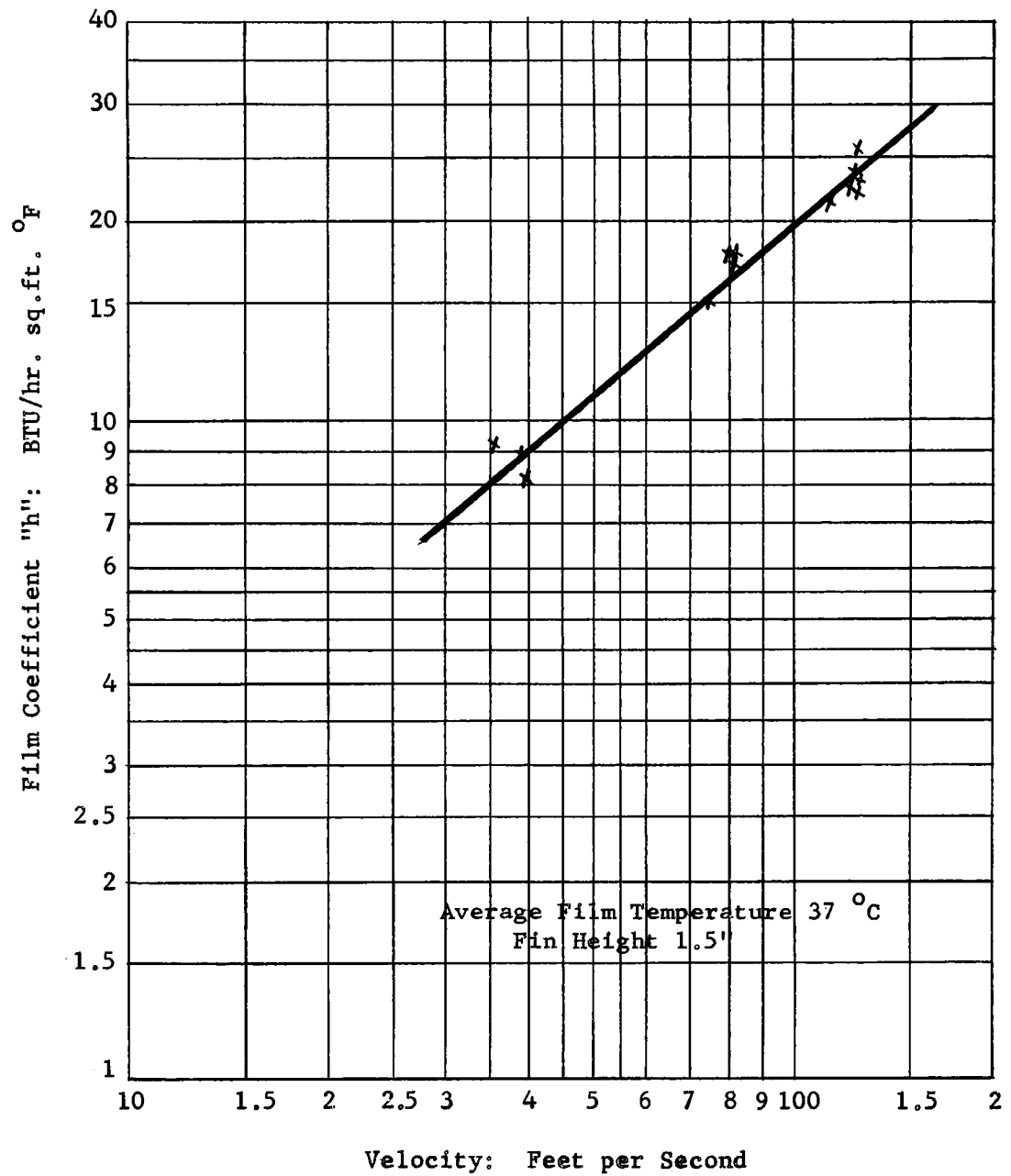


FIGURE (8)

FILM COEFFICIENT VS. VELOCITY

3/4" FIN SPACING

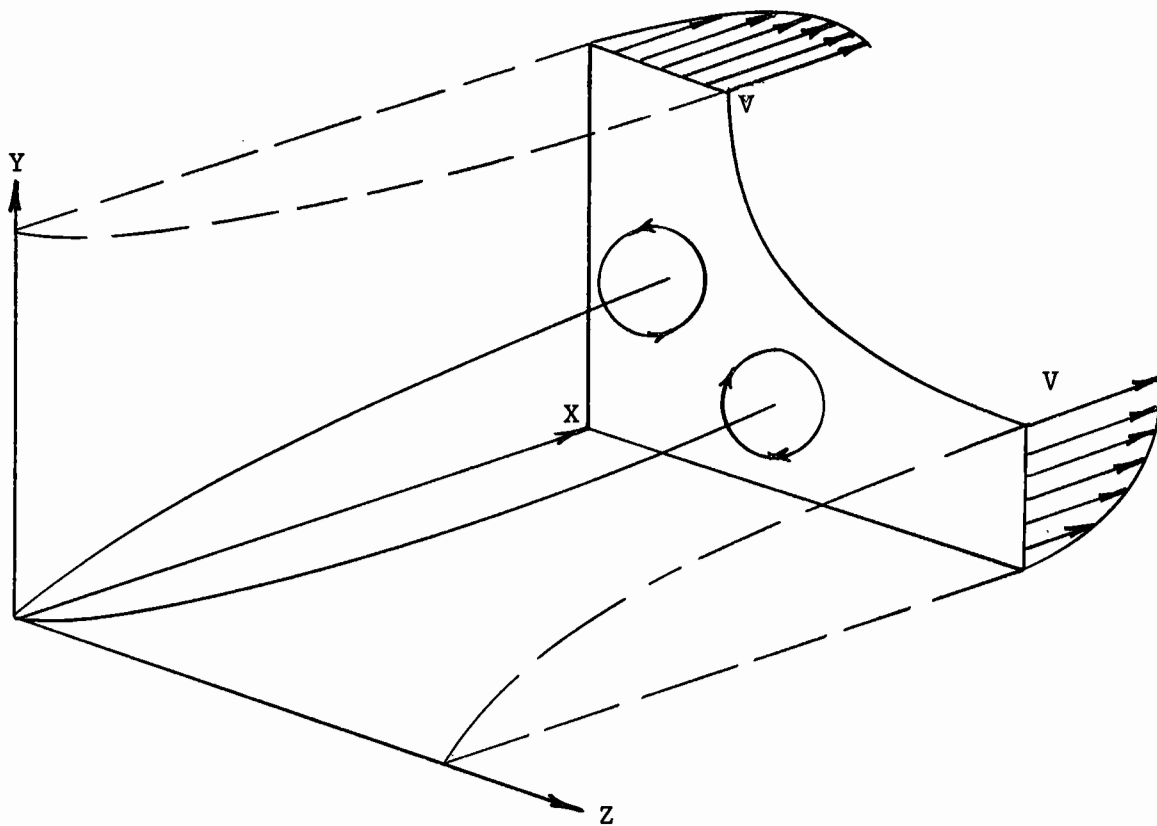


FIGURE (9)

BOUNDARY REGION AT THE INTERSECTION OF TWO PLANES

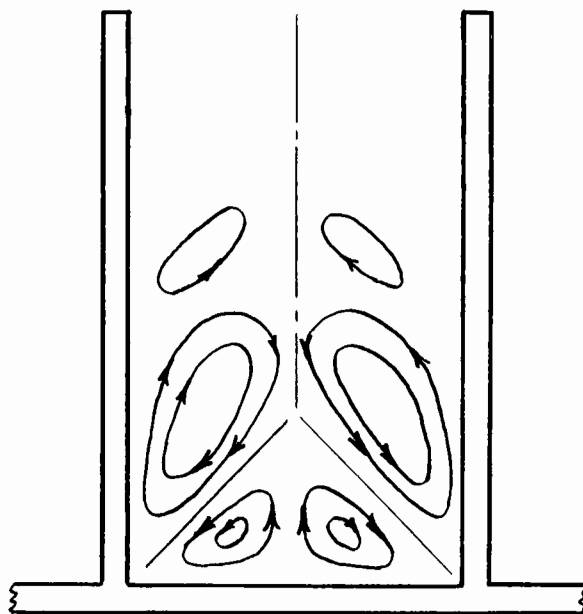


FIGURE (10)

SECONDARY FLOWS IN A RECTANGULAR CHANNEL

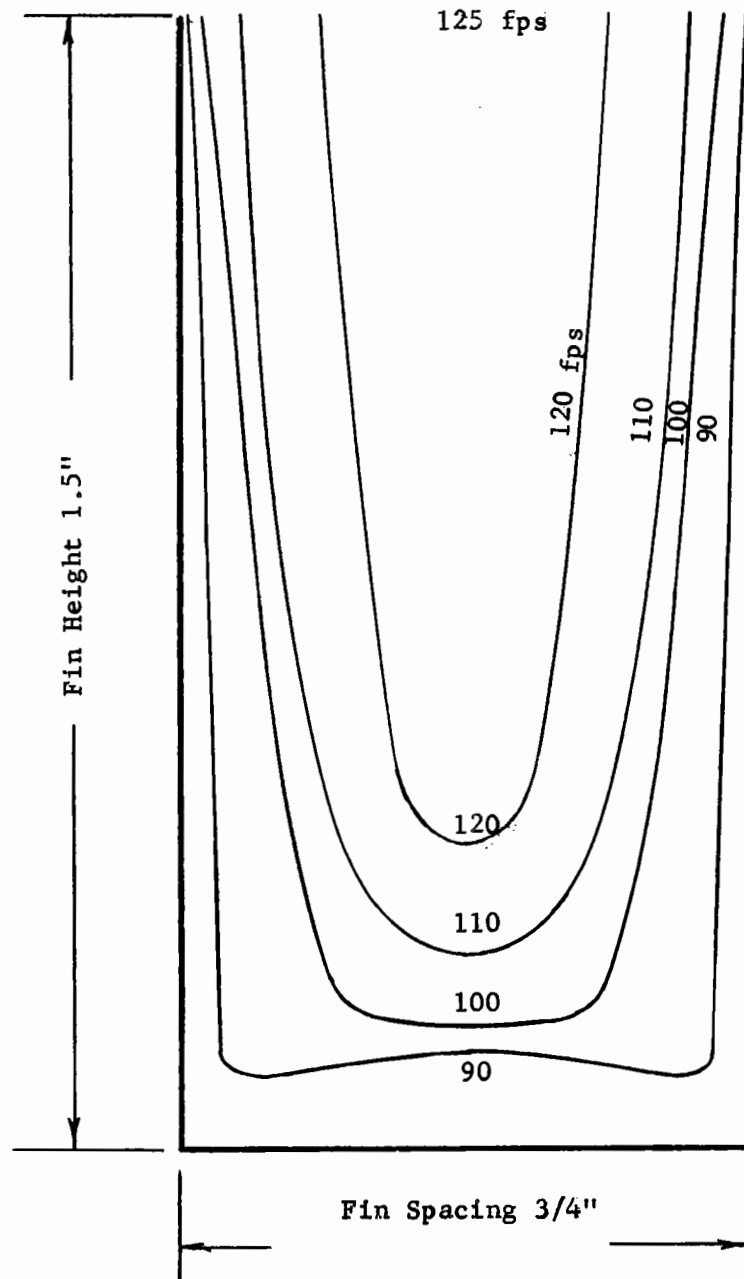


FIGURE (11)
CURVES OF CONSTANT VELOCITY
IN FIN CHANNEL